



The sensitivity of ground-level ozone to precursor emissions and source contributions in Southeast Asia

Jie Hu^{1,2}, David C. Wong^{3,4}, Jiaying Li^{1,2}, Tingting Fang^{1,5}, Steve H.L. Yim^{1,2,5,6*}

¹Centre for Climate Change and Environmental Health, Nanyang Technological University, Singapore 639798, Singapore

5 ²Asian School of the Environment, Nanyang Technological University, Singapore 639798, Singapore

³US Environmental Protection Agency, Research Triangle Park, NC, 27711, USA

⁴Department of Earth and Atmospheric Sciences, University of Houston, Houston, TX, 77204, USA

⁵Earth Observatory of Singapore, Nanyang Technological University, Singapore 639798, Singapore

⁶Lee Kong Chian School of Medicine, Nanyang Technological University, Singapore 639798, Singapore

10 *Correspondence to:* Steve H. L. Yim (yimsteve@gmail.com)

Abstract. To mitigate the surface ozone (O₃) pollution in Southeast Asia, a full understanding of the processes and contributions of precursor emissions [i.e., volatile organic compounds (VOCs) and nitrogen oxides (NO_x)] to O₃ is required but remains unclear. This study applied an adjoint sensitivity model to evaluate the source-receptor (S-R) relationship between O₃ and the precursors, as well as the source contributions over different receptor regions in Southeast Asia. The process analysis was performed to further characterize O₃ formation. We found a predominant NO_x-limited O₃ formation regime across Southeast Asia due to substantial regional biogenic VOC emissions, with exceptions in areas where anthropogenic NO_x emissions were significant, such as Singapore, Jakarta, Bangkok, and the Malacca Straits. NO_x was identified as the primary contributor to the surface O₃, whereas VOCs contributed positively to VOC-limited regions but negatively to NO_x-limited areas. Additionally, regional and super-regional transboundary air pollution accounted for 56-98% of surface O₃ concentration across Southeast Asian countries. The findings highlighted the need for differentiated O₃ mitigation strategies in Southeast Asia, combining coordinated regional NO_x emission reductions with targeted VOC controls in the VOC-limited urban areas.

1 Introduction

Ground-level ozone (O₃) is a major air pollutant that negatively impacts natural ecosystems and human health (Karlsson et al., 2017; Orru et al., 2013). From 2000 to 2019, global premature deaths attributed to excessive O₃ exposure increased



by 46%, from 290,000 to 423,000 (Malashock et al., 2022). O₃ is a secondary pollutant generated through complex photochemical reactions among O₃ precursors, namely nitrogen oxides (NO_x) and volatile organic compounds (VOCs) (Luecken et al., 2018; Qu et al., 2020). Mitigating O₃ pollution thus requires a full understanding of O₃ formation and removal. In some countries, previous efforts were put into controlling fine particulate matter (PM) levels by reducing their emissions. Despite the substantial reduction in PM levels, an increasing trend of O₃ was observed due to the changes in O₃ precursor emissions that unexpectedly enhanced O₃ formation (Kim et al., 2018; Li et al., 2019; Wang et al., 2019b). Proper management of O₃ pollution remained one of the challenges in air quality management. Accurately determining the sensitivity of O₃ to NO_x and VOCs and understanding its formation mechanisms are therefore essential in effectively controlling O₃ pollution.

Southeast Asia is characterized by a typical tropical climate with high temperature, intense sunlight, and frequent deep convection. In recent decades, this region has undergone rapid urbanization and industrialization (Behera & Dash, 2017), leading to increased anthropogenic emissions from transportation, energy generation, residential usage, and shipping (Ohara et al., 2007). The equatorward redistribution of anthropogenic emissions and the unique climate pattern account for a dramatic increase in O₃ in Southeast Asia. Observational studies have indicated a rising trend in surface O₃, with rates of 0.7-1.2 ppb per year over Peninsular Southeast Asia and 0.2-0.4 ppb per year over Maritime Southeast Asia from 2005 to 2016 (Wang et al., 2022a). Effectively addressing the O₃ pollution in Southeast Asia requires a comprehensive understanding of O₃ formation and transport dynamics, particularly the interactions between O₃ and its precursor emissions in the region.

Although numerous O₃ studies have been conducted in Southeast Asia recently (Amnuaylojaroen et al., 2014; Koike et al., 2013; Li et al., 2023a; Xing et al., 2021; Xue et al., 2021; Zhang et al., 2021), few studies have comprehensively evaluated the sensitivities of O₃ to NO_x and VOC emissions and their corresponding source contributions. One significant study analyzed twelve-year O₃ trends across Southeast Asia and found that growing anthropogenic emissions have driven large O₃ increases over Peninsular Southeast Asia (Wang et al., 2022a). Another important study focused on source apportionment, revealing that escalating NO_x emissions from transportation and international shipping were major contributors to the increase in tropospheric O₃ from 1990 to 2019 (Li et al., 2023c). While these studies effectively quantified the source apportionment of NO_x and VOCs from various sectors, the geographical distribution of O₃ sensitivity or the specific O₃ formation regimes remained unclear. Furthermore, other studies determined the O₃-NO_x-VOCs regimes (Marvin et al., 2020) and quantified the contribution of carbon monoxide (CO) and VOCs



(Amnuaylojaroen et al., 2019); however, they primarily concentrated on biomass-burning episodes (Xue et al., 2021),
55 neglecting anthropogenic emission sectors that contribute substantially to O₃ formation. Additionally, existing models
of O₃ formation regimes may not fully account for the transboundary source contributions from atmospheric processes,
which represent substantial O₃ levels in Southeast Asia. A comprehensive evaluation of O₃ sensitivities to NO_x and VOC
emissions and the source contribution is thus essential to thoroughly understand O₃ formation, transformation, and
removal in Southeast Asia.

60 Resolving the complex nonlinear chemical response of O₃ to precursor emissions remains a challenging endeavour
(Wang et al., 2019a). Current research on O₃ sensitivity to these emissions generally falls into four categories: empirical
kinetic modeling approach (Martinez et al., 1983). relative incremental reactivity (Carter, 1994; Martien et al., 2003).
photochemical indicators (Ren et al., 2022; Wang et al., 2021a). and air quality models (AQMs) (Dunker et al., 2020;
Dunker et al., 2002). Among these, AQMs are particularly pivotal as they estimate O₃ integration at each computational
65 step and assess sensitivity based on the changes in modeled species and input variables, such as the high-order
decoupled direct method (HDDM) (Estes et al., 2008; Kim, 2011) and adjoint techniques (Hakami et al., 2006; Pappin &
Hakami, 2013). Although HDDM has been employed to estimate O₃ sensitivity in Southeast Asia, its source-oriented
approach primarily considers the emission impacts from the entire region, which limits its application in providing
effective policy recommendations. In contrast, the receptor-oriented nature of the adjoint model allows for the precise
70 determination of O₃ sensitivity to specific location-based emission sources in a single simulation (Wang et al., 2019a).
Notably, the adjoint versions of GEOS-Chem (Henze et al., 2007; Zhang et al., 2011) and the Community Multiscale Air
Quality Modeling System (CMAQ) models (Zhao et al., 2020) were effectively used to simulate the sensitivities of O₃ to
its precursor emissions across various source regions and sectors (Wang et al., 2021b). These sensitivity models offer
opportunities to comprehensively evaluate O₃ sensitivity to its precursors' emissions.

75 Our study applied the CMAQ adjoint model to simulate the sensitivity of ground-level O₃ to the emissions in Southeast
Asia. Specifically, we investigated the ground-level O₃ response over the 11 countries in Southeast Asia to the NO_x and
VOC emission changes at each grid cell to identify the different influential pathways and calculated the source
contributions in Southeast Asia. To characterize the O₃ formation, we further utilized the process analysis technique to
apportion the contributions of each physical and chemical process. The methodology and model configuration of the
80 CMAQ-adjoint are described in Sect. 2. The O₃ concentration over Southeast Asia during four monsoon seasons is
presented in Sect. 3.1, the process analysis of O₃ formation is assessed in Sect. 3.2, the O₃ sensitivities to NO_x and VOC



emissions are shown in Sect. 3.3, and the source contributions over Southeast Asia and each receptor country are discussed in Sect. 3.4. An overall discussion is provided in Sect. 4.

2 Methods

85 The CMAQ modeling system (<https://www.epa.gov/cmaq>), developed by the U.S. Environmental Protection Agency (EPA), is a widely used chemical transport model (CTM) and was employed in this study. Further details about CMAQ can be found on the U.S. EPA's CMAS Centre website. The input meteorological data for our simulations were generated by the Weather Research and Forecasting (WRF) model version 3.7 (Skamarock et al., 2008). An extension of CMAQ, the CMAQ-adjoint model (Zhao et al., 2020), was used to calculate the source-receptor (S-R) relationships of O₃ to its precursors in a backward mode. This approach allowed us to determine the sensitivity of O₃ to emissions and to further estimate the contributions from various sources. The schematic flowchart of the study is shown in Fig. S1.

2.1 CMAQ model configuration

In this study, CMAQ v5.0.2 was used to simulate O₃ concentration. Both WRF and CMAQ were configured with a spatial resolution of 30 × 30 km. The domain covers Southeast Asia, as well as parts of South Asia and East Asia, and the study domain is illustrated in Fig. S2a. Southeast Asia is predominantly characterized by a tropical climate, with consistently high temperature (Fig. S2b), intense solar radiation, and elevated humidity throughout the year, along with substantial precipitation (Fig. S2c). The model domain was set with 26 vertical layers extending from the surface to the top level at 20 km at 50 hPa. For chemical processes, we utilized the CB05 (carbon bond version 5) gas-phase chemical mechanism and the AERO5 (aerosol module version 5), with photolysis rates calculated using the inline radiative transfer module.

The initial and boundary conditions were resampled from the GEOS-Chem global 3D Chemical Transport Model output, which had a spatial resolution of 5° × 4°. To ensure model stability and produce reliable estimates, a two-day spin-up period (Czader et al., 2013; Zhang et al., 2014) was implemented for each monsoon season in our simulation. Anthropogenic emissions over Southeast Asia were based primarily on the 2019 Copernicus Atmosphere Monitoring Service (CAMS) global inventory, which is constructed from EDGAR v5.0 annual emissions and applies monthly temporal profiles from CAMS-GLOB-TEMPO. For years beyond the latest EDGAR release, anthropogenic emissions were extended using sector- and country-specific trends from the Community Emissions Data System (CEDS) v2.0. Emissions were processed for nine source sectors, including transportation, shipping, industrial processes, residential,

biomass burning, power generation, refineries, solvent and fugitive sources, and agriculture (Granier et al., 2019).

110 Biogenic VOC emissions were estimated using the MEGAN v2.1 model (Guenther et al., 2012). To assess the influence of emission uncertainties on O₃ simulations, anthropogenic NO_x emissions were uniformly perturbed by $\pm 20\%$ and VOC emissions by $\pm 30\%$ (Fu et al., 2012; Kim et al., 2017). The resulting changes in regional surface O₃ concentration ranged from -1.5% to 1.5% for NO_x perturbations and from -3.9% to 4.2% for VOC perturbations (Table S1), indicating that the simulated O₃ concentration was relatively robust to reasonable uncertainties in precursor emissions.

115 In this study, both local and transboundary O₃ were evaluated across 12 receptor regions in Southeast Asia, encompassing 11 countries (Singapore, Malaysia, Indonesia, Brunei, Philippines, Cambodia, Myanmar, Vietnam, Thailand, Laos, and East Timor) and the entire Southeast Asia land region. We conducted the CMAQ simulations for 2019 to avoid potential influences of COVID-19 on emission patterns. Given that surface O₃ formation and transport are intricately linked to meteorological variations, and considering that O₃ concentration levels are significantly influenced by transboundary sources driven by the South Asian monsoon (Gao et al., 2020; Lu et al., 2018), our model simulations were conducted for January, April, July, and October of 2019 to represent the key meteorological changes in the winter monsoon, pre-summer monsoon, summer monsoon, and pre-winter monsoon seasons, respectively (Gu et al., 2024). The precursor emissions (Fig. S3) and seasonal meteorological conditions (Figs. S4 and S5) in 2019 were broadly consistent with their long-term patterns across Southeast Asia, suggesting that 2019 represents a reasonable baseline year for regional emissions and meteorology. We calculated the daily maximum 8-hour average O₃ concentration (MDA8) to represent the highest of the 8-hour average concentration levels for each day and aggregated them to the annual mean MDA8 O₃.

2.2 Process analysis

130 Process analysis in the CMAQ model is a diagnostic tool used to understand the contributions of various physical and chemical processes to atmospheric O₃ concentration. This study focused on Integrated Process Rate (IPR) analysis to assess O₃ formation through the selected processes, including gas-phase chemistry (CHEM), vertical diffusion (VDIF), horizontal diffusion (HDIF), horizontal advection (HADV), vertical advection (ZADV), cloud processes and aqueous chemistry (CLDS), and dry deposition (DDEP).



2.3 CMAQ-adjoint model

135 In this study, the CMAQ-adjoint was used to calculate the sensitivity of surface O₃ to the precursor emissions. The
adjoint model evaluates the gradient of a predefined cost function over the receptor region with respect to model inputs
through a single backward integration. Compared with the forward sensitivity methods (e.g., HDDM), which require
multiple forward simulations and are less efficient in resolving the responses to localized emissions of specific species,
the adjoint approach directly calculates the sensitivity of the cost function to emissions at every grid cell from a single
140 backward run. We set the cost function as the hourly O₃ concentration levels, and the receptor regions included the
entire continental Southeast Asia region and 11 countries within it. Therefore, 12 receptor regions were defined in
total, and each had the corresponding cost function and the adjoint simulation. Using this method, we computed the
non-linear partial derivatives of the hourly O₃ level to the emissions of all precursors and calculated backward during
the simulation. Specifically, the sensitivities of O₃ concentration to NO_x ($\frac{\partial O_{3m}}{\partial E_{i,j,NOx}}$) and VOCs ($\frac{\partial O_{3m}}{\partial E_{i,j,VOC}}$) were evaluated.
145 We considered VOC species included in the CB05 chemical mechanism (Table S2). Here, m denotes the defined
receptor region, E presents the precursor emissions, and i and j represent longitude and latitude indices of each grid cell,
respectively. The adjoint sensitivity ($\frac{\partial O_{3m}}{\partial E_{i,j}}$) therefore quantified the response of O₃ in the receptor region m to a
perturbation in precursor emissions of species (i.e., NO_x or VOCs) from a given grid cell (i, j), revealing how emission
perturbation from each location influences O₃ concentration levels in the receptor region. To improve interpretability
150 and enable the source contribution assessment, we further calculated semi-normalized sensitivity coefficients of O₃ with
respect to NO_x and VOC emissions:

$$\Phi_{O_{3m}-E_{i,j,NOx}} = \frac{\partial O_{3m}}{\partial E_{i,j,NOx}} \times E_{i,j,NOx}$$

$$\Phi_{O_{3m}-E_{i,j,VOC}} = \frac{\partial O_{3m}}{\partial E_{i,j,VOC}} \times E_{i,j,VOC}$$

Where O_{3m} denotes the O₃ concentration in the receptor region m , and $E_{i,j,NOx}$ and $E_{i,j,VOC}$ denote the precursor
155 emissions. Φ represents the semi-normalized sensitivity coefficients. In this way, $\Phi_{O_{3m}-E_{i,j,NOx}}$ and $\Phi_{O_{3m}-E_{i,j,VOC}}$
calculate the grid contributions of each precursor emission to the O₃ levels in the receptor regions.



2.4 Model evaluation

The WRF meteorological simulation in this study was evaluated against the ECMWF Reanalysis v5 (ERA5) monthly mean dataset for the four monsoon seasons (Text S1, Figs. S6-S9). The O₃ concentration levels simulated were validated against ground-level observations to assess model performance. O₃-level observations in Southeast Asia were obtained from the Acid Deposition Monitoring Network in East Asia (EANET) platform (<https://www.eanet.asia/>) and the Air Quality Historical Data Platform (AQI), created by the World Air Quality Project (<https://aqicn.org/data-platform/register>). In addition, due to the limited availability and sparse spatial coverage of ground-based O₃ observations in Southeast Asia, we further assessed the CMAQ O₃ simulation using the CAMS ECMWF Atmospheric Composition Reanalysis 4 (EAC4) monthly reanalysis product, which combined multi-source observations with data assimilation and provided a spatially complete benchmark for evaluating large-scale O₃ patterns in data-sparse regions. Model performance was rigorously evaluated using statistical assessments, including normalized mean bias (NMB), correlation coefficient (*r*), root mean square error (RMSE), and the index of agreement (IoA) between hourly observations and outputs from the CMAQ simulations (Kim et al., 2020).

3 Sensitivity of surface O₃ and source contributions

3.1 Simulation of O₃ concentration

The spatial distribution of simulated ground-level O₃ was evaluated using observations from 28 stations across Southeast Asia, including hourly measurements from six EANET stations and daily MDA8 O₃ records from 22 AQI stations. As shown in Fig. S10, most CMAQ simulations aligned within $\pm 50\%$ of the observations. The overall correlation (*r*) between hourly observed and simulated O₃ across the four months was 0.63, exceeding the benchmark criterion of $r > 0.5$ (Yang & Zhao, 2023). The NMB and IoA were 16.05% and 0.74, respectively. Detailed station-level evaluations are provided in Table S3, underscoring the reliability of the O₃ simulation in capturing the spatial variations in the region. Furthermore, due to the limited observations in Southeast Asia and differences in the spatial resolution between model simulations and ground measurements, our simulated O₃ distribution was further compared with the CAMS EAC4 reanalysis product for the four monsoon seasons (Fig. S11). The simulated O₃ showed good agreement with CAMS EAC4, showing consistent spatial patterns across Southeast Asia. In particular, the simulations captured regional hotspots with elevated O₃ levels over the coastal areas (e.g., Singapore, the Malacca Strait, and Jakarta) and lower concentration over northern Myanmar, Sumatra, and Borneo. Quantitative comparisons of NMB, *r*, and IoA for individual countries are summarized in Table S4. Singapore and East Timor were excluded due to their small spatial



185 extent, which could not be adequately represented by the coarse resolution (0.75°) of the EAC4 product. Overall, CMAQ showed strong consistency with CAMS EAC4. In addition, the scatter plots (Fig. S12) closely followed the 1:1 line, indicating that the simulations captured both the magnitude and spatial variability of surface O_3 in the reanalysis data.

The estimated annual mean MDA8 O_3 concentration over Southeast Asia in 2019 was 30.6 ppb, consistent with
190 observation-based estimates of approximately 30 ppb reported for the region ((Li et al., 2025b)). The seasonal averages were 33.2 ppb, 32.0 ppb, 28.6 ppb, and 28.4 ppb during the winter monsoon, pre-summer monsoon, summer monsoon, and pre-winter monsoon seasons, respectively. The seasonal distribution of MDA8 O_3 showed significant spatial and temporal variability across Southeast Asia (Fig. 1). Elevated O_3 levels were found in major coastal and urban regions, including Singapore, the Malacca Strait, Jakarta, Bangkok, Hanoi, Ho Chi Minh City, and Manila. These regions were
195 characterized by enhanced anthropogenic NO_x and VOC emissions (Figs. S13 and S14) from transportation, shipping, and industrial activities, which facilitated O_3 formation. At the country level, Singapore exhibited the highest annual mean MDA8 O_3 concentration (62.4 ppb), followed by Vietnam (41.7 ppb), Thailand (40.5 ppb), Cambodia (35.2 ppb), Laos (33.3 ppb), the Philippines (32.2 ppb), Myanmar (30.1 ppb), Malaysia (29.1 ppb), East Timor (28.8 ppb), Indonesia (26.5 ppb), and Brunei (20.3 ppb). Seasonal MDA8 O_3 levels across the four monsoon periods are summarized in Table
200 S5. The simulation results indicated higher regional O_3 levels during the winter monsoon season, particularly over the South China Sea, reflecting enhanced transboundary O_3 transport driven by northeasterly winds (Fig. S9a). In contrast, the lowest O_3 levels occurred during the summer monsoon, due to increased wet deposition associated with stronger rainfall under southwesterly winds (Fig. S9a). During the pre-summer and pre-winter monsoon seasons, O_3 levels were more strongly influenced by local emissions such as increased biomass burning (Fig. S15), resulting in elevated localized
205 O_3 concentration.

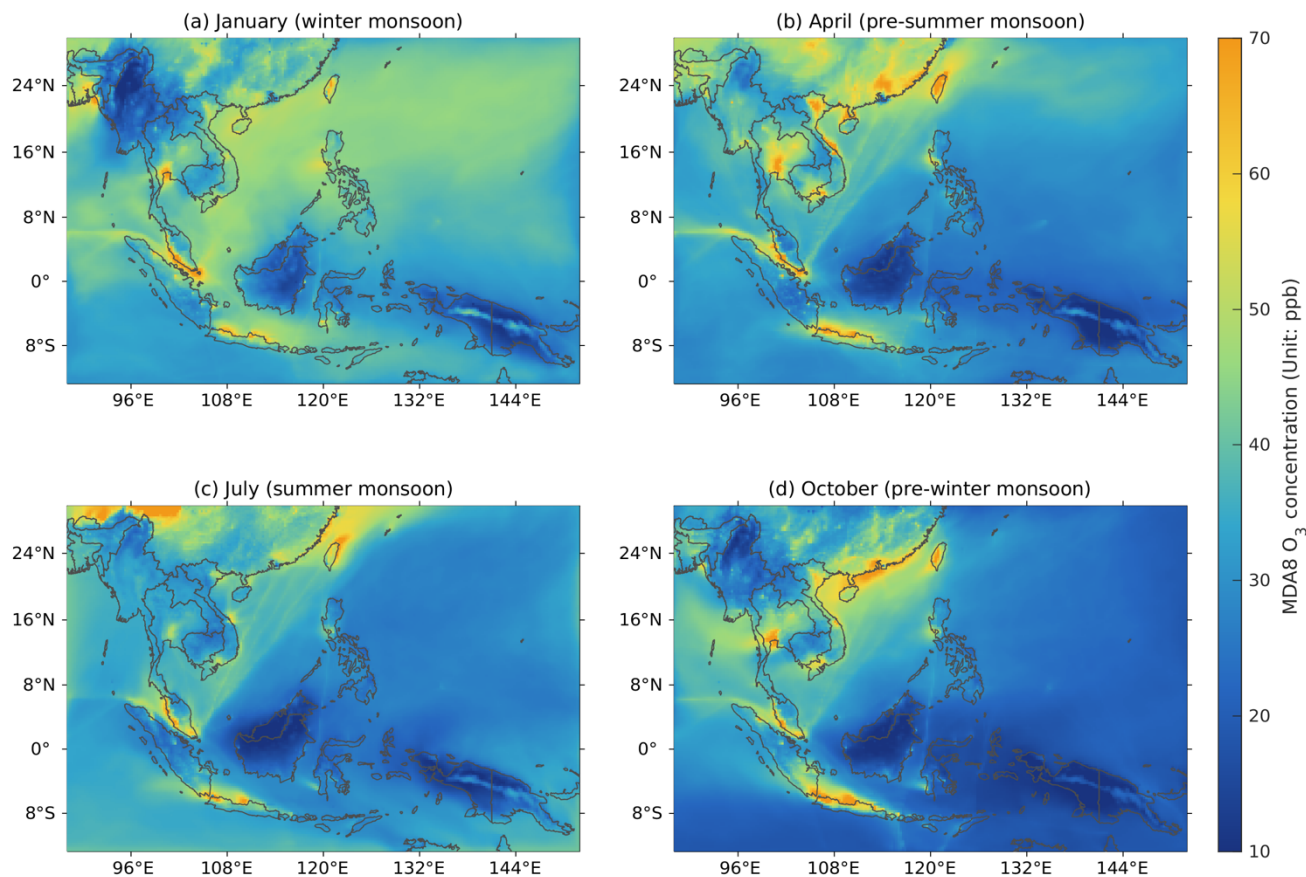


Figure 1: Spatial distribution of MDA8 O₃ levels in Southeast Asia during the four monsoon periods.

3.2 Process analysis of physical and chemical processes

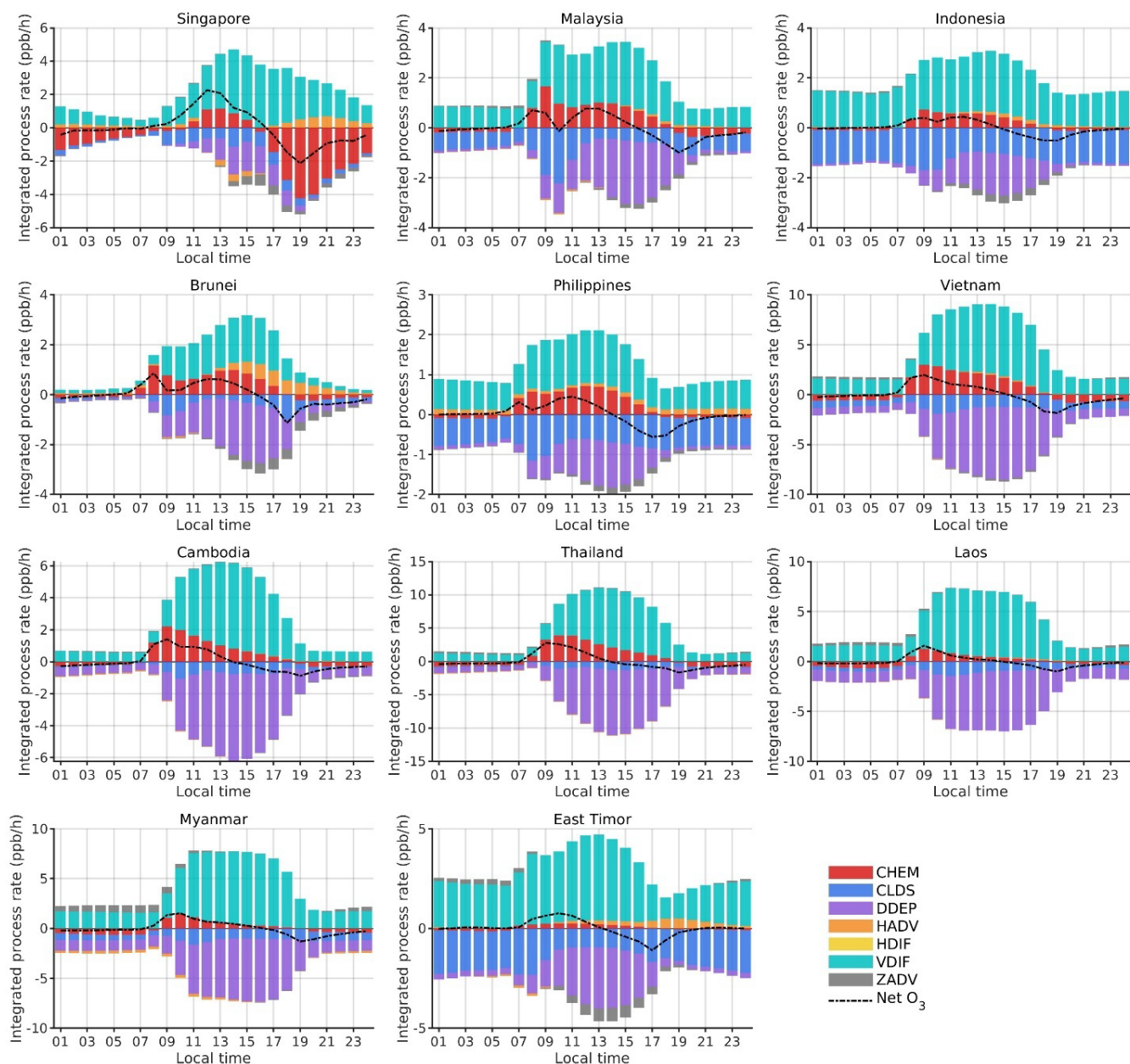
210 The Integrated Process Rate (IPR) at the surface level from the process analysis was examined to illustrate the contributions of different physical and chemical processes to ground-level O₃ formation across Southeast Asia (Fig. 2). Process contributions were calculated by averaging grid-level results at the national scale. From 09:00 to 16:00 local time, gas-phase chemistry provided a positive contribution in most Southeast Asian countries, facilitating O₃ formation. The magnitude of photochemical production varied substantially among countries. Thailand (15.7 ppb), Vietnam (12.6 ppb), and Cambodia (8.7 ppb) exhibited the largest contributions from gas-phase chemistry. In contrast, Singapore (-24.5 ppb) and Myanmar (0.36 ppb) showed relatively weaker photochemical O₃ production. Singapore represents a typical urban environment, where O₃ formation occurred under a VOC-limited regime (Fig. S16) with substantial anthropogenic NO_x emissions (Figs. S13 and S17). As shown in Figure S18, NO_x emissions were dominated by

215



transportation and shipping sources, with additional contributions from industry. Elevated NO_x levels and suppressed
220 O_3 production suggested strong NO titration, particularly during nighttime. In contrast, the relatively low O_3
production in Myanmar was mainly attributed to lower NO_x emissions (Figs. S17). Outside peak sunlight hours,
specifically before 07:00 and after 20:00 local time, gas-phase chemistry showed negative contributions across most
Southeast Asian countries (Fig. 2), reflecting the nighttime O_3 titration. The vertical distribution of individual processes
is further shown in Fig. S19, which presented the average contributions across 26 vertical layers from the surface to
225 approximately 20 km (Table S6) based on hourly simulations. The strongest chemical reactions occurred in the upper
layers, where photochemical activity was enhanced by stronger radiation and higher radical availability, resulting in
slightly larger contributions than those near the surface. In Singapore, the negative chemical contribution in the lowest
three layers (approximately 59 m, Table S6) was associated with strong near-surface O_3 titration.

In addition, vertical diffusion showed a positive contribution to surface O_3 in most Southeast Asian countries. The
230 process generally offset O_3 reductions caused by cloud processes, dry deposition, and O_3 titration. Temporally, the
influence of vertical diffusion increased after 8 am, coinciding with enhanced solar radiation and rising temperature,
which disrupted the stable nighttime atmosphere, allowing O_3 accumulated at higher altitudes to mix downwards to the
ground level. The contribution weakened after 18:00 as the atmosphere gradually stabilized with decreasing solar
radiation, limiting vertical mixing and trapping O_3 near the surface. Furthermore, Southeast Asia exhibited notably
235 higher contributions from cloud and aqueous processes compared to other regions (Wang et al., 2022b; Yang et al.,
2020), largely attributed to the proximity to the ocean, which provided abundant water vapor and frequent cloud cover.
The unique conditions reduced solar radiation reaching the surface and facilitated aqueous-phase reactions that
depleted O_3 and its precursors.



240 **Figure 2: Daily averaged variations of the physical and chemical contributions to the ground-level O₃ for 11 countries in Southeast Asia during the four monsoon seasons in 2019. The dotted line represents the net O₃ formation due to all atmospheric processes, and the columns show the average hourly contribution of each process, including gas-phase chemistry (CHEM), vertical diffusion (VDIF), horizontal diffusion (HDIF), horizontal advection (HADV), vertical advection (ZADV), cloud processes and aqueous chemistry (CLDS), and dry deposition (DDEP).**

245



3.3 Sensitivity of O₃ to precursor emissions

To further assess the response of ground-level O₃ to precursor emissions across Southeast Asia, we defined Southeast Asia as the receptor region and evaluated the sensitivities of O₃ to NO_x and VOC emissions from individual grid cells (Figs. 3 and 4). The strongest responses to NO_x emissions were observed during the pre-summer monsoon period in April (Fig. 3a), when meteorological conditions favoured photochemical O₃ production, including strong solar radiation (Fig. S20), elevated surface temperature (Fig. S21), and intensified biomass burning activities across mainland Southeast Asia (Fig. S22). The sensitivities also exhibited clear seasonal variations that were closely associated with the regional monsoon circulation (Fig. S9a). In particular, the spatial distribution of O₃ sensitivity closely followed the prevailing wind directions, with approximately 73.6% of high-sensitivity grid cells located in climatological upwind regions relative to Southeast Asia (Fig. S23). Emissions from these upwind regions influenced O₃ levels in Southeast Asia through multiple pathways ((Wang et al., 2019a)): (1) transport of O₃ precursors (NO_x and VOCs), which subsequently contributed to local photochemical O₃ production; (2) direct transport of O₃ formed in the source regions; and (3) photochemical O₃ formation occurring during the transport process, demonstrating that atmospheric transport played a critical role in the spatial distribution of O₃ sensitivity in Southeast Asia.

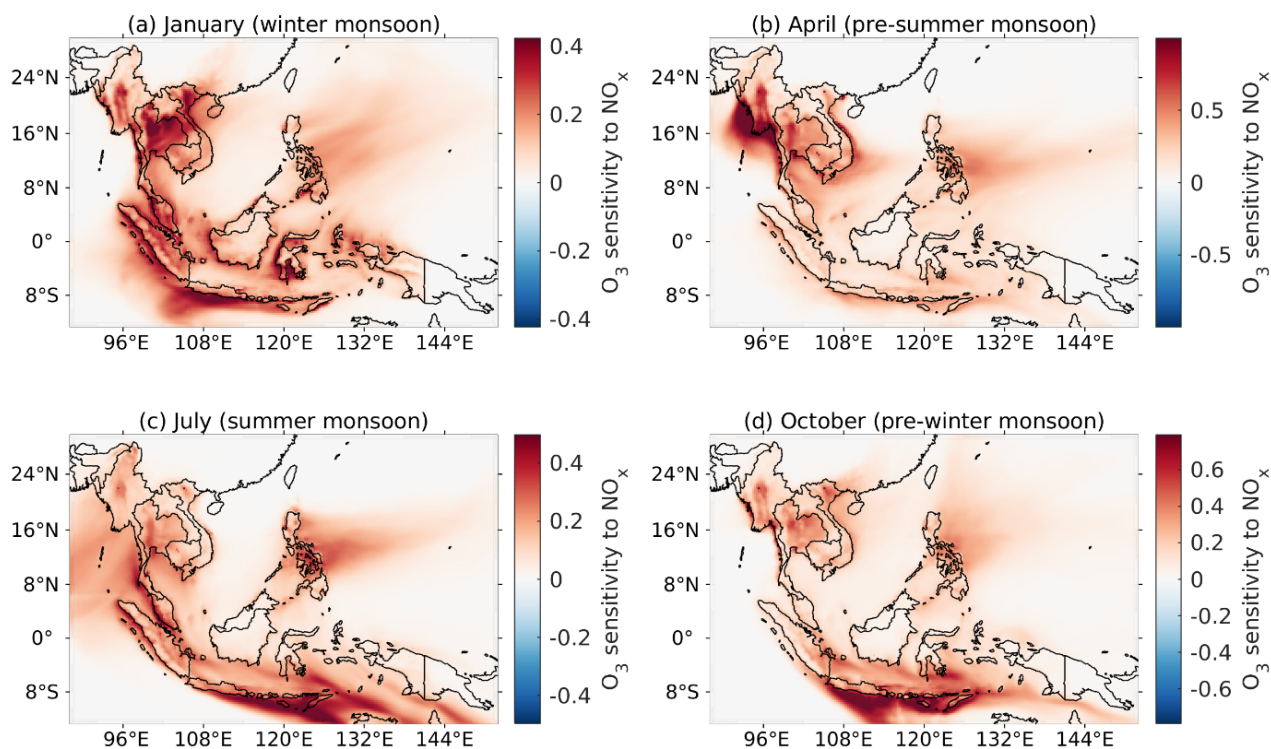
The O₃ sensitivity to NO_x emissions revealed a predominantly positive response across most of Southeast Asia, suggesting that increases in NO_x emissions generally led to higher surface O₃ concentration (Fig. 3). Elevated sensitivities were observed over central Myanmar, northern Thailand, northern Vietnam, and southern Malaysia, indicating that emissions from these regions could substantially enhance regional O₃ levels in Southeast Asia. High sensitivities were also found along coastal regions and major maritime shipping routes, particularly around the Malacca Strait, Java Island, coastal Vietnam, and the Philippine Sea. These areas represented locations where concentrated emissions (Fig. S13), together with efficient atmospheric transport (Fig. S9a), enhanced the regional O₃ response to NO_x emissions. It should be noted that although some highly urbanized regions were characterized by substantial NO_x emissions (Table S7) and VOC-limited chemical regimes (Fig. S16), they did not necessarily exhibit negative sensitivities to NO_x emissions. For example, cities such as Singapore, Bangkok, and Kuala Lumpur showed VOC-limited conditions but exhibited relatively weak positive sensitivities to NO_x emissions. Although substantial NO_x emissions in these urban areas may cause strong local O₃ titration, their influence on the regional O₃ response across Southeast Asia remained limited. Instead, NO_x emissions from these areas could be transported downwind and contributed to the photochemical O₃ production in surrounding regions. In such environments, O₃ formation was dominated by VOC emissions.

Conversely, O₃ sensitivity to VOC emissions was predominantly negative across Southeast Asia (Fig. 4), indicating that increases in VOC emissions generally led to lower O₃ concentration in most regions. Similar negative sensitivities have been reported in other NO_x-limited environments, such as northern California and the Great Smoky Mountains, where NO_x emissions are small and photochemical regimes are strongly NO_x-limited (Dunker et al., 2016; Hakami et al., 2004). The negative sensitivity in NO_x-limited areas arises from the reactions between O₃ and excess VOCs (e.g., isoprene) and their



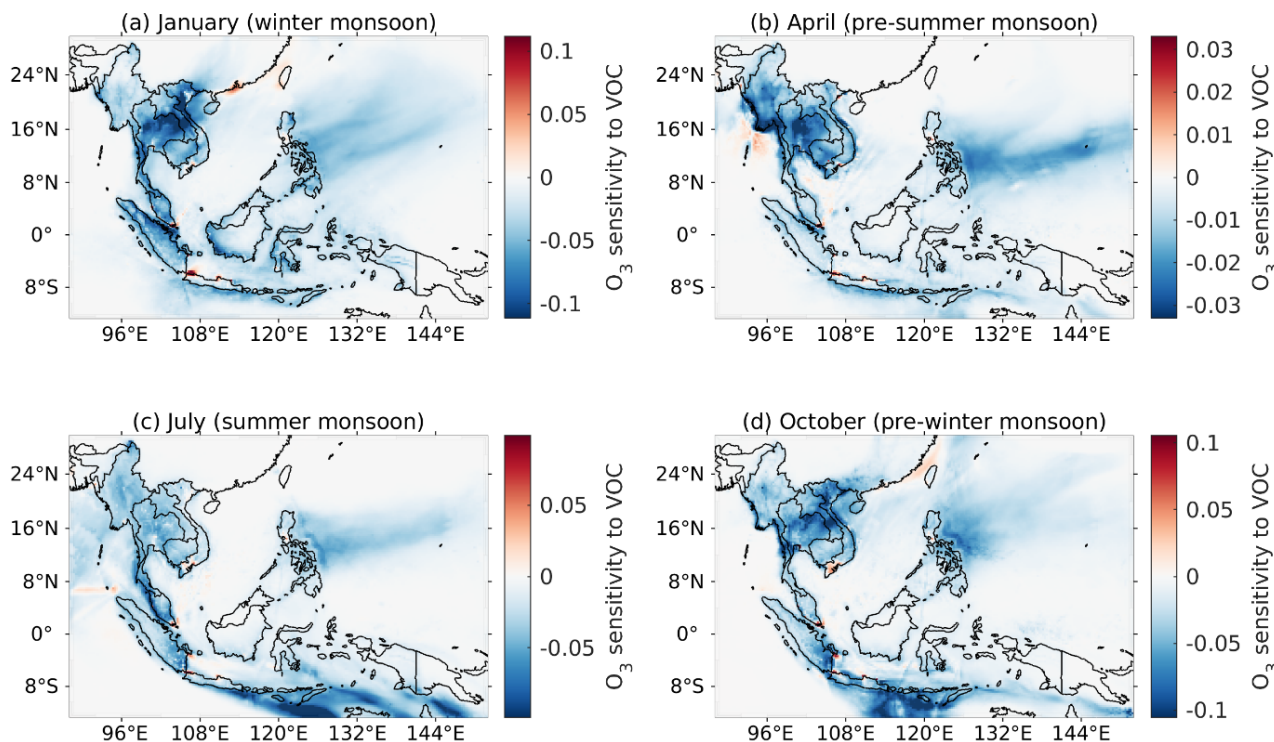
oxidative byproducts (Loreto et al., 2001). In contrast, regions characterized by VOC-limited chemical regimes (Fig. S16) exhibited positive sensitivities to VOC emissions, including coastal regions of China, the Malacca Strait, and major urban areas such as Bangkok, Singapore, Hanoi, and Jakarta. In these environments, O₃ formation was more determined by VOC availability, and VOC emissions enhanced photochemical O₃ production. Overall, the magnitudes of O₃ sensitivity to VOC emissions (Fig. 4) were generally smaller than the sensitivity to NO_x emissions (Fig. 3), which is consistent with the widespread dominance of NO_x-limited regimes across Southeast Asia (Fig. S16).

To assess the sensitivity of O₃ concentration in Southeast Asian countries to precursor emissions, the receptor regions were further defined as individual countries in Southeast Asia. The sensitivities to NO_x emissions generally exhibited positive patterns (Figs. S24-34), and their spatial distributions closely followed the prevailing wind directions. For instance, in the Philippines, O₃ sensitivities to NO_x emissions were consistently positive, and the spatial patterns aligned well with the wind directions during the four monsoon seasons. Negative O₃ sensitivities to NO_x emissions were mainly observed in highly urbanized regions such as Singapore, which was characterized by VOC-limited chemical regimes (Table S7). The negative sensitivities indicated that increasing NO_x emissions reduced net O₃ production, primarily because elevated NO concentration enhanced O₃ titration. In contrast, the sensitivities to VOC emissions exhibited positive values in the urban areas, indicating that VOC emissions in those urban regions contributed positively to O₃ concentration in the corresponding receptor countries.



295

Figure 3: Spatial distribution of the monthly mean sensitivity of O_3 in Southeast Asia to NO_x emissions during the four monsoon seasons. Among them, the red colour depicts positive sensitivity, while the blue colour represents negative sensitivity. Unit: ppb/mol^{-5} .



300 **Figure 4: Spatial distribution of the monthly mean sensitivity of O_3 in Southeast Asia to VOC emissions during the four monsoon seasons. Among them, the red colour depicts positive sensitivity, while the blue colour represents negative sensitivity. Unit: ppb/mol^{-s} .**

3.4 Relative source contributions to surface O_3

305 The adjoint-based grid-level impacts of NO_x and VOC emissions on O_3 concentration across Southeast Asia (Fig. S35) and the 11 receptor countries (Fig. S36) were assessed using semi-normalized adjoint sensitivity coefficients, obtained by multiplying the adjoint sensitivities by the corresponding emissions. NO_x emissions predominantly contributed positively to O_3 concentration (Fig. S37), whereas VOC emissions generally reduced O_3 levels in the region (Fig. S38). Notably, both the geographic extent and magnitude of NO_x impacts were greater than those of VOCs, highlighting the dominant role of NO_x in

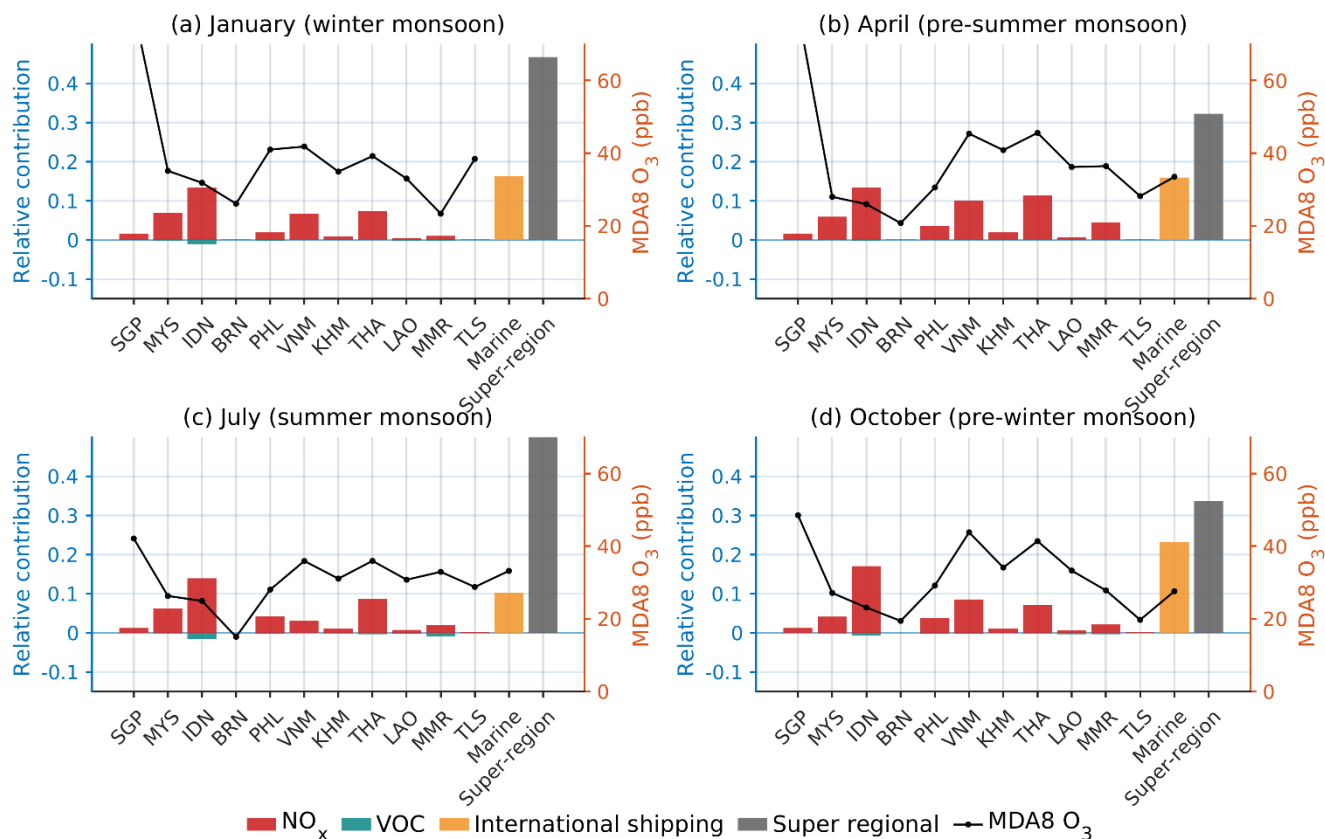
310 influencing the regional O_3 levels in Southeast Asia. Based on the adjoint sensitivities, the grid-level results directly represented the O_3 contributions from the precursor emissions at each grid cell, indicating that reductions in precursor emissions would correspondingly influence O_3 concentration depending on the local chemical regime. Distinct spatial variations were observed between urban and rural regions. Despite the effect of NO titration, precursor emissions in urban and suburban areas generally enhanced O_3 concentration. In contrast, negative O_3 responses were found in most rural areas,

315 largely attributable to strong NO_x -limited conditions where high biogenic VOC emissions reduced O_3 levels.

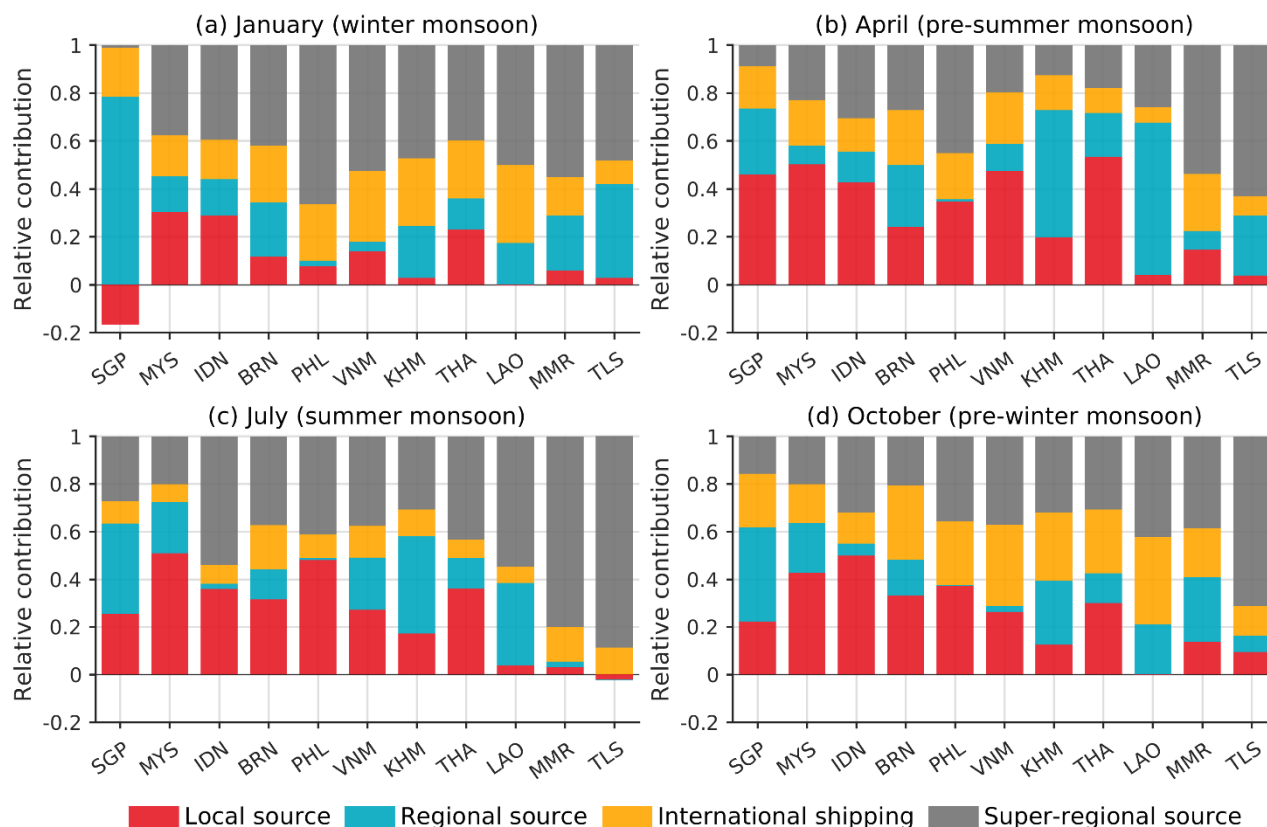


The contributions to O₃ concentration in Southeast Asia from individual countries, international shipping, and super-regional sources were further quantified (Fig. 5). Source contributions were aggregated at the grid level for each receptor area and then aggregated as percentages of the total contributions from all sources within the study domain. Regional sources included emissions from other Southeast Asian countries, while super-regional sources represented land regions outside Southeast Asia and the boundary conditions of the modeling domain. The relative contributions indicated that NO_x was the dominant precursor influencing O₃ levels in Southeast Asia. Among the Southeast Asian countries, Indonesia, Vietnam, and Thailand contributed the most, accounting for 4.1%, 2.1%, and 1.7% of the O₃ concentration in the region, respectively. International shipping also made substantial contributions, ranging from 10.2% in July to 23.2% in October. In addition, super-regional sources represented the largest contribution overall, accounting for 46.7%, 32.2%, 52.3%, and 33.6% during the four monsoon seasons, respectively.

The relative contributions of local emissions, regional transport within Southeast Asia, international shipping, and super-regional sources to O₃ concentration across Southeast Asian countries are presented in Fig. 6. The results indicated a substantial influence of transboundary O₃ across the region, particularly during the winter monsoon in January, when regional transport, international shipping, and super-regional sources accounted for 22.9%, 22.0%, and 45.5% of O₃ levels on average, respectively. The strong transboundary influence reflected both regional transport across Southeast Asia and long-range inflow from surrounding continental regions, in addition to background O₃ and precursor transport from outside the modeling domain. On average, transboundary source accounts for 80.6% of O₃ concentration in Singapore, 56.7% in Malaysia, 60.6% in Indonesia, 74.9% in Brunei, 68.1% in the Philippines, 71.3% in Vietnam, 86.9% in Cambodia, 64.4% in Thailand, 98.2% in Laos, 90.7% in Myanmar, and 96.5% in East Timor. Local emissions contributed between 1.8% in Laos and 43.5% in Malaysia, whereas regional sources ranged from 1.1% in the Philippines to 45.8% in Singapore, indicating that O₃ levels in Singapore were strongly influenced by emissions from neighbouring countries. Contributions from international shipping varied from 10.4% in East Timor to 24.6% in Vietnam. Super-regional sources exhibited the largest variability, accounting for 17.3% in Singapore and up to 68.4% in East Timor. The super-regional influence was further divided into boundary-driven background O₃ and long-range transport of precursor emissions from outside Southeast Asia. The boundary contribution ranged from 0.37 ppb in Brunei to 14.7 ppb in East Timor, while transported super-regional emissions contributed between 3.5 ppb in East Timor and 10.9 ppb in the Philippines (Table S8), highlighting the substantial influence of super-regional sources on concentration and associated public health impacts in Southeast Asia.



345 **Figure 5:** Source contributions of NO_x and VOCs from different countries and regions to O_3 concentration (unit: ppb) in Southeast Asia during the four monsoon seasons. SGP: Singapore, MYS: Malaysia, IDN: Indonesia, BRN: Brunei, PHL: Philippines, VNM: Vietnam, KHM: Cambodia, THA: Thailand, LAO: Laos, MMR: Myanmar, TLS: East Timor.



350 **Figure 6: Local, regional, and super-regional source contributions of NO_x and VOCs across countries in Southeast Asia during the four monsoon seasons. SGP: Singapore, MYS: Malaysia, IDN: Indonesia, BRN: Brunei, PHL: Philippines, VNM: Vietnam, KHM: Cambodia, THA: Thailand, LAO: Laos, MMR: Myanmar, TLS: East Timor.**

4 Discussion and conclusions

Although surface O_3 has been extensively investigated in North America, Europe, and East Asia, its characteristics in Southeast Asia differed markedly from those in mid-latitude regions, particularly in terms of chemical regime, controlling factors, and transport pathways. In China, high O_3 levels were mainly concentrated in northern and eastern megacity clusters, where strong local photochemical production led to elevated summer O_3 and predominantly VOC-limited or transitional regimes (Li et al., 2025a; Ren et al., 2022). In the United States and Europe, surface O_3 generally declined after 2000, and the regional chemical regime increasingly shifted toward NO_x -limited conditions under long-term precursor emission reductions, although the VOC-limited regime persisted in some urban areas (Nelson & Drysdale, 2025). In contrast, Southeast Asia showed a predominantly NO_x -limited regime under a tropical monsoon environment. However, unlike in the United States and Europe, where NO_x -limited conditions were mainly driven by substantial anthropogenic emission reductions (Li et al., 2023b), it was associated with high biogenic VOC emissions across the Southeast Asian region. Southeast Asia also differed from other regions in its stronger dependence on monsoon-driven transboundary transport (Fang



365 et al., 2025). Unlike North America and Europe, where background O_3 was often influenced by intercontinental transport, wildfires, or stratospheric intrusion (Jaffe et al., 2018), the spatial patterns of O_3 concentration and precursor sensitivities in Southeast Asia were closely aligned with monsoon circulation, indicating that source-receptor relationships were highly seasonally dependent. In addition, deep convection, frequent precipitation, and strong cloud and aqueous processes further distinguished Southeast Asia from other regions by influencing regional O_3 production, transport, and removal. Despite rapid
370 emission growth and increasing population exposure in recent decades, a comprehensive assessment of O_3 sensitivity and formation processes in Southeast Asia remained limited. Therefore, a receptor-oriented evaluation of O_3 source-receptor relationships in Southeast Asia was critical not only for supporting local and regional policy design but also for filling a critical gap in the global O_3 research landscape. By integrating CMAQ adjoint sensitivity analysis with process analysis, our study provided a receptor-oriented evaluation of surface O_3 sensitivity to grid-level precursor emissions and quantified O_3
375 source contributions across four representative monsoon seasons. The findings showed surface O_3 in Southeast Asia was influenced by both local photochemical productions and substantial transboundary transport, improving the interpretability of O_3 formation and advancing broader understanding of O_3 control effectiveness in tropical monsoon environments.

Our sensitivity results indicated that most of Southeast Asia was characterized by a NO_x -limited photochemical regime, consistent with previous long-term regime assessments based on OMI satellite products (Amnuaylojaroen et al., 2019). In
380 contrast, urban areas such as Singapore, the Malacca Straits, Jakarta, Bangkok, Hanoi, and Manila were identified as VOC-limited or transitional regimes, reflecting the combined influence of elevated anthropogenic emissions and strong NO titration in the urban hotspots. The regime variations implied the geographically differentiated mitigation strategies in Southeast Asia. For VOC-limited environments, reducing VOC emissions is advisable to effectively lower surface O_3 , while NO_x reductions alone may weaken NO titration (Wang et al., 2019b) and hence increase O_3 concentration. Nevertheless,
385 because NO_x remains an important precursor for secondary $PM_{2.5}$ formation (Blanchard & Hidy, 2005; Wang et al., 2017), coordinated reductions of both VOC and NO_x were recommended in VOC-limited regions to jointly mitigate O_3 and $PM_{2.5}$ burdens, resulting in co-benefits. To reduce VOC emissions, we highlighted the targeted controls on anthropogenic sources, particularly from transportation and industry, which accounted for the majority of anthropogenic VOC emissions (Table S7) in the typical VOC-limited regions. Conversely, for NO_x -limited regions covering most parts of Southeast Asia (e.g., rural
390 Indonesia, rural Malaysia, and mountainous regions of mainland Southeast Asia), NO_x -prioritized emission reductions were suggested to yield effective O_3 benefits. For instance, we recommended reducing emissions from transportation and shipping in Malaysia, whereas transportation and industry emissions should be highlighted in mountainous mainland Southeast Asian regions, where they contributed substantially to regional-scale NO_x burdens (Table S9). The specific emission controls suggested that O_3 mitigation could be effectively integrated with broader clean-energy and decarbonization strategies, such
395 as the adoption of green energy and low-emission technologies to reduce the O_3 precursors in the region.



The process analysis identified vertical diffusion, gas-phase chemistry, and horizontal advection as the three dominant processes contributing to surface O_3 in Southeast Asia, consistent with our adjoint sensitivity results showing that regional O_3 levels were largely determined by transboundary contributions. Specifically, the Philippines, Myanmar, and East Timor were particularly affected by super-regional pollution due to their proximity to the surrounding seas, whereas Singapore, Cambodia, and Laos experienced substantial regional influences associated with adjacency to the neighbouring countries with high precursor emissions. The predominance of transboundary O_3 indicated elevated background O_3 levels and substantial inequities in O_3 control effectiveness across Southeast Asian countries, as downwind receptors may experience high O_3 exposure despite relatively low emissions, thereby reducing the effectiveness of local mitigation efforts. Our findings underscored the need for a collaborative regional emission reduction framework to reduce O_3 pollution and improve public health across the region.

By using the adjoint model, we assessed the sensitivity of surface O_3 to precursor emissions and quantified the O_3 source contributions from each grid cell, which enabled us to track how emissions from different locations and species affected O_3 in receptor regions. In this study, receptors were defined as both the entire Southeast Asia domain and individual countries, allowing us to evaluate how grid-level emissions influenced O_3 concentration at regional and national scales. For instance, by defining Thailand as the receptor region, our results showed that emissions from Bangkok accounted for approximately 4.2% of Thailand's local-source contribution to O_3 pollution, providing quantitative evidence to support targeted mitigation strategies. As a receptor-oriented approach, the adjoint model not only quantified grid-level source contributions but also identified the emission areas where O_3 concentration were most sensitive to. It is therefore suggested to employ the adjoint-based framework for health-oriented emission controls (Hu et al., 2026), enabling broader use in air quality management and improving public health.

Our study also has several limitations. First, the relatively sparse monitoring network in Southeast Asia limited the evaluation of simulated surface O_3 . To complement the comparisons, global surface O_3 reanalysis data were used to assess the spatial consistency of the simulations. Future improvements in model evaluation would benefit from expanded ground-based monitoring networks and the integration of satellite-derived O_3 products. Second, the model resolution of 30 km may not fully resolve sub-grid urban processes such as NO titration. Nevertheless, O_3 is fundamentally a regional-scale pollutant, and its formation and distribution are strongly influenced by large-scale transport and regional photochemistry rather than local-scale processes alone. In this study, the simulated negative NO_x sensitivities over major urban centers (e.g., Singapore) suggested that the regional sensitivity patterns were reasonably captured. Additionally, the focus of this study was on O_3 formation and transport in the Southeast Asian region, which were mainly driven by regional circulation and chemical processes. The 30 km resolution was sufficient to capture the main spatial patterns of O_3 and its sensitivity to precursor emissions. More detailed urban-scale titration effects could be more



accurately represented by defining receptor regions at the city scale in future studies. Despite the limitations, this work provided the first comprehensive assessment of source-receptor relationships between surface O₃ and grid-level precursor emissions across Southeast Asia, offering useful insights for both local and regional O₃ mitigation strategies.

430 **Data availability**

All the raw data used are publicly available.

Supplement link

The link to the supplement will be included by Copernicus, if applicable.

Author contributions

435 Jie Hu: Methodology, Data curation, Software, Validation, Formal analysis, Investigation, Writing - Original Draft, Visualization; David C. Wong: Software, Validation, Formal analysis, Writing - Review & Editing; Jiaying Li: Software, Formal analysis; Tingting Fang: Formal analysis, Writing - Review & Editing; Steve H.L. Yim: Conceptualization, Formal analysis, Resources, Writing - Review & Editing, Supervision, Project administration, Funding acquisition.

Competing interests

440 The authors declare no competing interests.

Disclaimer

The views expressed in this article are those of the author(s) and do not necessarily represent the views or the policies of the U.S. Environmental Protection Agency.

Acknowledgements

445 The authors would like to acknowledge the High-Performance Computing Centre of Nanyang Technological University (Singapore) for providing the computing resources, facilities, and services that have contributed substantially to this work.

<https://doi.org/10.5194/egusphere-2026-2148>

Preprint. Discussion started: 8 May 2026

© Author(s) 2026. CC BY 4.0 License.



Financial support

This work was jointly supported by the Ministry of Education, Singapore, under its MOE AcRF Tier 3 Award MOET32022-0006, by Tsao Family Foundation and by Dr. Stephen Riady Geoscience Scholars Fund (023923-00001).

450 **Review statement**

The review statement will be added by Copernicus Publications listing the handling editor as well as all contributing referees according to their status anonymous or identified.



References

455

Amnuaylojaroen, T., Barth, M., Emmons, L., Carmichael, G., Kreasuwun, J., Prasitwattanaseree, S., & Chantara, S.: Effect of different emission inventories on modeled ozone and carbon monoxide in Southeast Asia, *Atmospheric Chemistry and Physics*, 14, 12983-13012, 2014.

460

Amnuaylojaroen, T., Macatangay, R. C., & Khodmanee, S.: Modeling the effect of VOCs from biomass burning emissions on ozone pollution in upper Southeast Asia, *Heliyon*, 5, 2019.

Behera, S. R., & Dash, D. P.: The effect of urbanization, energy consumption, and foreign direct investment on the carbon dioxide emission in the SSEA (South and Southeast Asian) region, *Renewable and Sustainable Energy Reviews*, 70, 96-106, 2017.

465

Blanchard, C. L., & Hidy, G. M.: Effects of SO₂ and NO_x emission reductions on PM_{2.5} mass concentrations in the southeastern United States, *Journal of the Air & Waste Management Association*, 55, 265-272, 2005.

Carter, W. P.: Development of ozone reactivity scales for volatile organic compounds, *Air & waste*, 44, 881-899, 1994.

Czader, B. H., Li, X., & Rappenglueck, B.: CMAQ modeling and analysis of radicals, radical precursors, and chemical transformations, *Journal of Geophysical Research: Atmospheres*, 118, 11,376-311,387, 2013.

470

Dunker, A. M., Koo, B., & Yarwood, G.: Ozone sensitivity to isoprene chemistry and emissions and anthropogenic emissions in central California, *Atmospheric environment*, 145, 326-337, 2016.

Dunker, A. M., Wilson, G., Bates, J. T., & Yarwood, G.: Chemical sensitivity analysis and uncertainty analysis of ozone production in the comprehensive air quality model with extensions applied to Eastern Texas, *Environmental Science & Technology*, 54, 5391-5399, 2020.

475

Dunker, A. M., Yarwood, G., Ortmann, J. P., & Wilson, G. M.: Comparison of source apportionment and source sensitivity of ozone in a three-dimensional air quality model, *Environmental science & technology*, 36, 2953-2964, 2002.

Estes, M., Koo, B., Yarwood, G., & Cohan, D. S.: Higher-Order Decoupled Direct Method (HDDM) for Ozone Modeling Sensitivity Analyses and Code Refinements, 2008.

Fang, T., Hu, J., Gu, Y., Sung, J. J., & Yim, S. H. L.: Response of ozone to current and future emission scenarios and the resultant human health impact in Southeast Asia, *Environment International*, 197, 109333, 2025.

480

Fu, J. S., Dong, X., Gao, Y., Wong, D. C., & Lam, Y. F.: Sensitivity and linearity analysis of ozone in East Asia: The effects of domestic emission and intercontinental transport, *Journal of the Air & Waste Management Association*, 62, 1102-1114, 2012.

Gao, M., Gao, J., Zhu, B., Kumar, R., Lu, X., Song, S., Zhang, Y., Jia, B., Wang, P., & Beig, G.: Ozone pollution over China and India: seasonality and sources, *Atmospheric Chemistry and Physics*, 20, 4399-4414, 2020.

485

Granier, C., Darras, S., van Der Gon, H. D., Jana, D., Elguindi, N., Bo, G., Michael, G., Marc, G., Jalkanen, J.-P., & Kuenen, J. (2019). *The Copernicus atmosphere monitoring service global and regional emissions (April 2019 version)* [Copernicus Atmosphere Monitoring Service].

Gu, Y., Fang, T., & Yim, S. H. L.: Source emission contributions to particulate matter and ozone, and their health impacts in Southeast Asia, *Environment International*, 186, 108578, 2024.

490

Guenther, A., Jiang, X., Heald, C. L., Sakulyanontvittaya, T., Duhl, T. a., Emmons, L., & Wang, X.: The Model of Emissions of Gases and Aerosols from Nature version 2.1 (MEGAN2. 1): an extended and updated framework for modeling biogenic emissions, *Geoscientific Model Development*, 5, 1471-1492, 2012.

Hakami, A., Bergin, M. S., & Russell, A. G.: Ozone formation potential of organic compounds in the eastern United States: A comparison of episodes, inventories, and domains, *Environmental science & technology*, 38, 6748-6759, 2004.

495

Hakami, A., Seinfeld, J. H., Chai, T., Tang, Y., Carmichael, G. R., & Sandu, A.: Adjoint sensitivity analysis of ozone nonattainment over the continental United States, *Environmental science & technology*, 40, 3855-3864, 2006.

Henze, D. K., Hakami, A., & Seinfeld, J. H.: Development of the adjoint of GEOS-Chem, *Atmospheric Chemistry and Physics*, 7, 2413-2433, 2007.

500

Hu, J., Fang, T., & Yim, S. H.: Apportioning the ozone-related health impact to precursor emissions and formulating health-oriented ozone control strategies in Southeast Asia, *Journal of Environmental Management*, 401, 128780, 2026.



- Jaffe, D. A., Cooper, O. R., Fiore, A. M., Henderson, B. H., Tonnesen, G. S., Russell, A. G., Henze, D. K., Langford, A. O., Lin, M., & Moore, T.: Scientific assessment of background ozone over the US: Implications for air quality management, *Elem Sci Anth*, 6, 56, 2018.
- 505 Karlsson, P. E., Klingberg, J., Engardt, M., Andersson, C., Langner, J., Karlsson, G. P., & Pleijel, H.: Past, present and future concentrations of ground-level ozone and potential impacts on ecosystems and human health in northern Europe, *Science of the total Environment*, 576, 22-35, 2017.
- Kim, C.-H., Lee, S.-H., Jang, M., Chun, S., Kang, S., Ko, K.-K., Lee, J.-J., & Lee, H.-J.: A Study on statistical parameters for the evaluation of regional air quality modeling results-Focused on fine dust modeling, *Journal of Environmental Impact Assessment*, 29, 272-285, 2020.
- 510 Kim, E., Kim, B.-U., Kim, H. C., & Kim, S.: The variability of ozone sensitivity to anthropogenic emissions with biogenic emissions modeled by MEGAN and BEIS3, *Atmosphere*, 8, 187, 2017.
- Kim, J., Ghim, Y. S., Han, J.-S., Park, S.-M., Shin, H.-J., Lee, S.-B., Kim, J., & Lee, G.: Long-term trend analysis of Korean air quality and its implication to current air quality policy on ozone and PM 10, *Journal of Korean Society for Atmospheric Environment*, 34, 1-15, 2018.
- 515 Kim, S.-T.: Estimating ozone sensitivity coefficients to NO_x and VOC emissions using BFM and HDDM for a 2007 June episode, *Journal of Environmental Science International*, 20, 1465-1481, 2011.
- Koike, T., Watanabe, M., Hoshika, Y., Kitao, M., Matsumura, H., Funada, R., & Izuta, T.: Effects of ozone on forest ecosystems in East and Southeast Asia, *Developments in Environmental Science*, 13, 371-390, 2013.
- 520 Li, H., Yang, Y., Jin, J., Wang, H., Li, K., Wang, P., & Liao, H.: Climate-driven deterioration of future ozone pollution in Asia predicted by machine learning with multi-source data, *Atmospheric Chemistry and Physics*, 23, 1131-1145, 2023a.
- Li, K., Jacob, D. J., Liao, H., Zhu, J., Shah, V., Shen, L., Bates, K. H., Zhang, Q., & Zhai, S.: A two-pollutant strategy for improving ozone and particulate air quality in China, *Nature Geoscience*, 12, 906-910, 2019.
- 525 Li, K., Tan, R., Qiao, W., Lee, T., Wang, Y., Zhang, D., Tang, M., Zhao, W., Gu, Y., & Fan, S.: Surface and tropospheric ozone over East Asia and Southeast Asia from observations: distributions, trends, and variability, *Atmospheric Chemistry and Physics*, 25, 11575-11596, 2025a.
- Li, K., Tan, R., Qiao, W., Lee, T., Wang, Y., Zhang, D., Tang, M., Zhao, W., Gu, Y., Fan, S., Zhang, J., Lyu, X., Xue, L., Xu, J., Ma, Z., Latif, M. T., Amnuaylojaroen, T., Gil, J., Lee, M. H., Bak, J., Kim, J., Liao, H., Kanaya, Y., Lu, X., Nagashima, T., & Koo, J. H.: Surface and tropospheric ozone over East Asia and Southeast Asia from observations: distributions, trends, and variability, *EGUsphere*, 2025, 1-38, <https://doi.org/10.5194/egusphere-2024-3756>, 2025b.
- 530 Li, P., Yang, Y., Wang, H., Li, S., Li, K., Wang, P., Li, B., & Liao, H.: Source attribution of near-surface ozone trends in the United States during 1995–2019, *Atmospheric Chemistry and Physics*, 23, 5403-5417, 2023b.
- Li, S., Yang, Y., Wang, H., Li, P., Li, K., Ren, L., Wang, P., Li, B., Mao, Y., & Liao, H.: Rapid increase in tropospheric ozone over Southeast Asia attributed to changes in precursor emission source regions and sectors, *Atmospheric Environment*, 304, 119776, 2023c.
- 535 Loreto, F., Mannozi, M., Maris, C., Nascetti, P., Ferranti, F., & Pasqualini, S.: Ozone quenching properties of isoprene and its antioxidant role in leaves, *Plant Physiology*, 126, 993-1000, 2001.
- Lu, X., Zhang, L., Liu, X., Gao, M., Zhao, Y., & Shao, J.: Lower tropospheric ozone over India and its linkage to the South Asian monsoon, *Atmospheric Chemistry and Physics*, 18, 3101-3118, 2018.
- 540 Luecken, D., Napelenok, S., Strum, M., Scheffe, R., & Phillips, S.: Sensitivity of ambient atmospheric formaldehyde and ozone to precursor species and source types across the United States, *Environmental science & technology*, 52, 4668-4675, 2018.
- Malashock, D. A., Delang, M. N., Becker, J. S., Serre, M. L., West, J. J., Chang, K.-L., Cooper, O. R., & Anenberg, S. C.: Global trends in ozone concentration and attributable mortality for urban, peri-urban, and rural areas between 2000 and 2019: a modelling study, *The Lancet Planetary Health*, 6, e958-e967, 2022.
- 545 Martien, P. T., Harley, R. A., Milford, J. B., & Russell, A. G.: Evaluation of incremental reactivity and its uncertainty in southern California, *Environmental science & technology*, 37, 1598-1608, 2003.
- Martinez, J. R., Maxwell, C., Javitz, H. S., & Bawol, R.: Performance evaluation of the Empirical Kinetic Modeling Approach (EKMA), *Air Pollution Modeling and Its Application II*, 199-211, 1983.



- 550 Marvin, M. R., Palmer, P. I., Latter, B. G., Siddans, R., Kerridge, B. J., Latif, M. T., & Khan, M. F.: Photochemical environment over Southeast Asia primed for hazardous ozone levels with influx of nitrogen oxides from seasonal biomass burning, *Atmospheric Chemistry and Physics Discussions*, 2020, 1-33, 2020.
- Nelson, B. S., & Drysdale, W. S.: Urban ozone trends in Europe and the USA (2000–2021), *Atmospheric Chemistry and Physics*, 25, 16009-16026, 2025.
- 555 Ohara, T., Akimoto, H., Kurokawa, J.-i., Horii, N., Yamaji, K., Yan, X., & Hayasaka, T.: An Asian emission inventory of anthropogenic emission sources for the period 1980–2020, *Atmospheric Chemistry and Physics*, 7, 4419-4444, 2007.
- Orru, H., Andersson, C., Ebi, K. L., Langner, J., Åström, C., & Forsberg, B.: Impact of climate change on ozone-related mortality and morbidity in Europe, *European Respiratory Journal*, 41, 285-294, 2013.
- 560 Pappin, A. J., & Hakami, A.: Attainment vs exposure: Ozone metric responses to source-specific NO_x controls using adjoint sensitivity analysis, *Environmental science & technology*, 47, 13519-13527, 2013.
- Qu, H., Wang, Y., Zhang, R., & Li, J.: Extending ozone-precursor relationships in China from peak concentration to peak time, *Journal of Geophysical Research: Atmospheres*, 125, e2020JD033670, 2020.
- Ren, J., Guo, F., & Xie, S.: Diagnosing ozone–NO_x–VOC sensitivity and revealing causes of ozone increases in China based on 2013–2021 satellite retrievals, *Atmospheric Chemistry and Physics*, 22, 15035-15047, 2022.
- 565 Skamarock, W. C., Klemp, J. B., Dudhia, J., Gill, D. O., Barker, D. M., Duda, M. G., Huang, X.-Y., Wang, W., & Powers, J. G.: A description of the advanced research WRF version 3, NCAR technical note, 475, 10.5065, 2008.
- Wang, M., Yim, S. H., Wong, D., & Ho, K.: Source contributions of surface ozone in China using an adjoint sensitivity analysis, *Science of the Total Environment*, 662, 385-392, 2019a.
- 570 Wang, N., Lyu, X., Deng, X., Huang, X., Jiang, F., & Ding, A.: Aggravating O₃ pollution due to NO_x emission control in eastern China, *Science of the Total Environment*, 677, 732-744, 2019b.
- Wang, W., van der A, R., Ding, J., van Weele, M., & Cheng, T.: Spatial and temporal changes of the ozone sensitivity in China based on satellite and ground-based observations, *Atmospheric chemistry and physics*, 21, 7253-7269, <https://doi.org/10.5194/acp-21-7253-2021>, 2021a.
- 575 Wang, X., Fu, T.-M., Zhang, L., Cao, H., Zhang, Q., Ma, H., Shen, L., Evans, M. J., Ivatt, P. D., & Lu, X.: Sensitivities of ozone air pollution in the Beijing–Tianjin–Hebei area to local and upwind precursor emissions using adjoint modeling, *Environmental Science & Technology*, 55, 5752-5762, 2021b.
- Wang, X., Fu, T. M., Zhang, L., Lu, X., Liu, X., Amnuaylojaroen, T., Latif, M. T., Ma, Y., Zhang, L., & Feng, X.: Rapidly changing emissions drove substantial surface and tropospheric ozone increases over Southeast Asia, *Geophysical Research Letters*, 49, e2022GL100223, 2022a.
- 580 Wang, Y., Xue, Y., Tian, H., Gao, J., Chen, Y., Zhu, C., Liu, H., Wang, K., Hua, S., & Liu, S.: Effectiveness of temporary control measures for lowering PM_{2.5} pollution in Beijing and the implications, *Atmospheric Environment*, 157, 75-83, 2017.
- Wang, Y., Yaluk, E. A., Chen, H., Jiang, S., Huang, L., Zhu, A., Xiao, S., Xue, J., Lu, G., & Bian, J.: The importance of NO_x control for peak ozone mitigation based on a sensitivity study using CMAQ-HDDM-3D model during a typical episode over the Yangtze River Delta region, China, *Journal of Geophysical Research: Atmospheres*, 127, e2022JD036555, 2022b.
- 585 Xing, L., Bei, N., Guo, J., Wang, Q., Liu, S., Han, Y., Pongpiachan, S., & Li, G.: Impacts of biomass burning in peninsular Southeast Asia on PM_{2.5} concentration and ozone formation in Southern China During Springtime—A case study, *Journal of Geophysical Research: Atmospheres*, 126, e2021JD034908, 2021.
- 590 Xue, L., Ding, A., Cooper, O., Huang, X., Wang, W., Zhou, D., Wu, Z., McClure-Begley, A., Petropavlovskikh, I., & Andreae, M. O.: ENSO and Southeast Asian biomass burning modulate subtropical trans-Pacific ozone transport, *National Science Review*, 8, nwaal32, 2021.
- Yang, J., & Zhao, Y.: Performance and application of air quality models on ozone simulation in China—A review, *Atmospheric Environment*, 293, 119446, 2023.
- 595 Yang, X., Wu, K., Wang, H., Liu, Y., Gu, S., Lu, Y., Zhang, X., Hu, Y., Ou, Y., & Wang, S.: Summertime ozone pollution in Sichuan Basin, China: Meteorological conditions, sources and process analysis, *Atmospheric Environment*, 226, 117392, 2020.



- 600 Zhang, H., Chen, G., Hu, J., Chen, S.-H., Wiedinmyer, C., Kleeman, M., & Ying, Q.: Evaluation of a seven-year air quality
simulation using the Weather Research and Forecasting (WRF)/Community Multiscale Air Quality (CMAQ)
models in the eastern United States, *Science of the Total Environment*, 473, 275-285, 2014.
- Zhang, L., Jacob, D. J., Downey, N. V., Wood, D. A., Blewitt, D., Carouge, C. C., van Donkelaar, A., Jones, D. B., Murray,
L. T., & Wang, Y.: Improved estimate of the policy-relevant background ozone in the United States using the
605 GEOS-Chem global model with $1/2 \times 2/3$ horizontal resolution over North America, *Atmospheric Environment*, 45,
6769-6776, 2011.
- Zhang, Y., West, J. J., Emmons, L. K., Flemming, J., Jonson, J. E., Lund, M. T., Sekiya, T., Sudo, K., Gaudel, A., & Chang,
K. L.: Contributions of world regions to the global tropospheric ozone burden change from 1980 to 2010,
Geophysical Research Letters, 48, e2020GL089184, 2021.
- 610 Zhao, S., Russell, M. G., Hakami, A., Capps, S. L., Turner, M. D., Henze, D. K., Percell, P. B., Resler, J., Shen, H., &
Russell, A. G.: A multiphase CMAQ version 5.0 adjoint, *Geoscientific model development*, 13, 2925-2944, 2020.